From

Huda Jameel Makki Al-Khafaji
Research Scholar,
Department of Studies and Research in Biochemistry
Mangalore University P G Centre, Jnana Kaveri campus,
Chikka Aluvara, Kodagu District, Karnataka -571 232.

To

The Registrar (Evaluation)
Mangalore University
Mangalagangothri- 574 199

Through

1. The Research Guide,

Department of Studies and Research in Biochemistry.

.

2. **The Chairman,**

Department of Studies and Research in Biochemistry,

Dear Sir,

Sub: Submission of the synopsis for conducting pre-thesis submission collequium

With respect to the abovesubject, I would like to bring to your notice that I Huda Jameel Makki working as research scholar (Provisional Registration No.: **188145503**) Department of Studies and Research in Biochemistry PG Centre, Jnana Kaveri Campus, Chikka Aluvara. Under the guidance of **prof. K S C Chandrashekharaiah** I have completed my research work colloquim entitled "**Green synthesis of Nano-particles using medicinal plants and evaluation for anti-cancer activity against Leukemia cells**" for your kind perusal and consideration. Therefore, I kindly request you to conduct pre-thesis submission colloquium and do the needful.

Thank you

Your faithfully

Huda Jameel Makki

MANGALORE UNIVERSITY

PRE-THESIS SUBMISSION COLLOQUIUM SYNOPSIS

Title

"Green synthesis of Nano-particles using medicinal plants and evaluation for anti-cancer activity against Leukemia cells"

Submitted

By

Ms. Huda Jameel Makki Al-khafaji

Research scholar, Department of studies and research in Biochemistry

Mangalore University P.G. Centre, Jnana Kaveri campus, Kodagu

Provisional Registration No: 188145503

Under the Guidance of

Prof. KS Chandrashekharaiah

Dept. of Studies in Biochemistry, Mangalore University

Jnan Kaveri Campus, Chikka Aluvara, Kodagu District, Karnataka-571232

September - 2019

Chapter 1 Introduction:-

Nanoparticles (NPs) are a new influence in the therapeutic industry. In spite of the pertinacious efforts in the study of NPs., Green synthesis of metal nanoparticles offers an environmental-friendly approach to synthesize NPs. NPs can be reduced to metal ions in a one-step eco-friendly process, called green synthesis, by secondary metabolites. The synthetic process of NP synthesis often requires stabilizing and capping agents, which can be overcome by green production of nanoparticles from plant extracts that produces biologically active molecules.

Cancer continues to be a top cause of death globally regardless the considerable advancements made in its study, understanding, and treatment. In the fight against cancer, early diagnosis and screening are crucial components that enable better treatment outcomes and lower cancer death rates. Although we can now treat a variety of cancers with traditional chemotherapy, there are still issues with its usage, including low absorption and multidrug resistance, along with a lack of selective targeting to cancer (Phan & Haes., 2019).

Instead, targeted therapy employs therapeutic and anti-cancer medicines that can specifically target genes and proteins essential for the survival of cancer cells that can form tumors (Andleeb et al., 2021). Through the bloodstream injections of microparticles and nanoparticles, are often administered to solid tumors (Yang et al., 2019). Green gold nanoparticles (AuNPs) and silver nanoparticles (AgNPs) look to be a potential approach for specifically targeting lethal medications to malignant cells, although it has not yet been well researched.

When synthesizing NPs as carriers or cytotoxic agents, there are numerous factors to take into account. It is vital to build delivery platforms that can react to a variety of stimuli since the regulated release of medications in organs, tissues, or cells does not follow Fick's equations of diffusion. AuNPs and AgNPs are effective anticancer agents that are becoming more selective to cancer cells (Yang G., 2019).

Molecular probes, biosensors, and targeted delivery vehicles are the principal uses for greenly produced AuNPs (Rostami & Sazgarnia., 2019). Green biogenic AgNPs are also widely known for having antibacterial properties. Although bacterial resistance to AgNPs has recently been discovered, cationic silver (Ag^{+}) resistance has long been known to exist. The

efficacy of AgNPs in the therapy of various cancers has also been established (Gomes et al., 2021). AgNPs' anticancer capabilities work through several methods, including as the release of silver ions and the creation of intracellular free radicals, which result in the dysregulation of vital cellular processes, cell damage, and death. These characteristics of AuNPs and AgNPs are intriguing and significant because they may help us overcome the problems associated with chemotherapy, including poor bioavailability, side effects from high doses, non-specific targeting, and the emergence of drug resistance (Neouze & Schubert., 2008).

Objectives:-

- Green synthesis of Metal Nano-particles using selected medicinal plants.
- Screening of metal nanoparticles for anticancer activity against Leukemia.
- Evaluation of nano-particles for anticancer activity against Leukemia cell lines.
- *In vivo* efficacy study of selected Nano-particles in Leukemia xenograft rat model.

Chapter 2 LITERATURE REVIEW:-

Nanoparticles, ranging from 1 to 100 nanometres in size, are a crucial element of nanotechnology. The particles have distinctive physical, chemical, and biological characteristics because of their greater surface area, heightened reactivity, and improved mechanical strength. Nanoparticles can exist in many dimensions (0D, 1D, 2D, or 3D) and shapes (spherical, cylindrical, tubular, conical, or irregular). Surfaces can be either uniform or uneven, and they may consist of crystalline or amorphous single or multi-crystal solids (Ealia and Saravanakumar., 2017).

Green synthesis of nanoparticles using medicinal plants

Medicinal plants contain various phytochemicals such as alkaloids, flavonoids, terpenoids, and phenolic compounds that can reduce and stabilize metal ions leading to the formation of nanoparticles. The green synthesis has several advantages over conventional methods. Firstly, it is a cost-effective method that uses readily available plant extracts as reducing and stabilizing agents. Secondly, it is an eco-friendly method that does not utilize toxic chemicals and solvents, thereby reducing the risk of environmental pollution. Thirdly, it is a simple and efficient method that does not require complex equipment or specialized expertise.

Several studies have reported the successful synthesis of nanoparticles using medicinal plants. For example, Azadirachta indica leaf extract has been used for the green synthesis of silver nanoparticles, which exhibited antimicrobial activity against various pathogenic bacteria (Bhat, *et al*., 2019). Similarly, Curcuma pseudomontana isolated curcumin has been used for the green synthesis of gold nanoparticles, which exhibited antioxidant and anti-inflammatory properties (Muniyappan, *et al*., 2021).

Several studies have reported the green synthesis of nanoparticles using medicinal plants and their characterization using various analytical techniques, such as UV-Vis spectroscopy, X-ray diffraction, and transmission electron microscopy. For instance, (Kumarasamyraja, *et al*., 2013) synthesized silver nanoparticles (AgNPs) using the leaf extract of Acalypha indica and characterized them using UV-Vis spectroscopy and X-ray diffraction. They reported that the synthesized AgNPs were spherical and exhibited excellent antimicrobial activity against various bacterial strains. Further research is needed to explore the potential of medicinal plants for the green synthesis of nanoparticles and their applications in various fields.

Anti-cancer activity of nanoparticles synthesized using medicinal plants

Nanoparticles synthesized using medicinal plants have shown significant anti-cancer activity against leukemia cells both *in vitro* and *in vivo*. The Jurkat cell line is a well-established model for studying leukemia and has been used extensively for evaluating the anti-cancer activity of various compounds, including nanoparticles. Several studies have evaluated the anti-cancer activity of nanoparticles synthesized using medicinal plants against leukemia cells/Jurkat cell line. For instance, (Ghozali, *et al*., 2015) the synthesized C. roseus-AgNPs shows higher toxicity effects compared to C. roseus aqueous extract on both cell types, both treatments are more effective in inhibiting Jurkat cells compared to HT-29 cell. The anti-cancer activity of these nanoparticles is attributed to their ability to induce apoptosis, inhibit cell proliferation, and modulate the expression of various genes and proteins involved in the regulation of cell cycle and apoptosis. For instance, silver nanoparticles synthesized using Aloe vera showed significant anti-cancer activity against leukemia cells by inducing apoptosis and inhibiting cell proliferation (Siddiqi, *et al*., 2018).

Recent research has focused on the use of upregulation of genes p53 and caspase 3 as a potential new approach to treating leukemia. The p53 gene is a tumor suppressor gene that

plays a key role in preventing the development of cancer. Caspase 3 is a protease enzyme that is involved in programmed cell death, or apoptosis. Upregulation of these genes may promote apoptosis of leukemia cells, leading to their destruction.Studies have shown that upregulation of p53 and caspase 3 can enhance the efficacy of chemotherapy in treating leukemia. For example, a study by (Kojima, *et al*.,2005) found that upregulation of p53 and caspase 3 increased the sensitivity of leukemia cells to the chemotherapy drug cytarabine. Similarly, a study by (Xu.Z, *et al*., 2018) demonstrated that upregulation of caspase 3 enhanced the effectiveness of the chemotherapy drug decitabine in treating acute myeloid leukemia.

Eventually, green synthesis of nanoparticles using medicinal plants has emerged as a promising approach for the synthesis of nanoparticles with potential biomedical applications. Several studies have reported the green synthesis of nanoparticles using medicinal plants and their evaluation for anti-cancer activity against leukemia cells/Jurkat cell line. The results of these studies suggest that nanoparticles synthesized using medicinal plants exhibit excellent anti-cancer activity against leukemia cells and have the potential to be developed as effective anti-cancer agents. However, further studies are needed to evaluate the toxicity and biocompatibility of these nanoparticles *in vivo* before they can be translated to clinical applications.

Chapter 3: Method and materials and results of Green synthesis of Metal Nano-particles using selected medicinal plants.

Plant specimens used in the study: *Ocimum sanctum, Asparagus racemous, Azardirachta indica, Citrus lemon* and *Phyllanthus emblica*

Qualitative and quantitative phytochemical analysis was carried out to screen for the presence of major phytochemicals like Alkaloids, Flavonoids, Terpenes, Saponins, tannins, glycosides, phenols, Carboxylic acids etc. from the plants.

Quantitative Analysis of Phytochemicals: Total alkaloids (Ajanal, *et al*., 2012), Total flavonoids (Kumar, et al., 2014), Total phenolics, (Madhu, *et al*., 2016) and total tannins (Kumar, *et al*., 2014) were estimated using standard methods. Capsaicin, Quercetin, gallic acid and tannic acid were used as standards for alkaloids, flavonoids, phenloics and tannins respectively.

Phytochemical analysis: Qualitative phytochemical analysis revealed the existence of Alkaloid, Carbohydrate, Phenolics, Terpenoid Glycoside Steroid Saponin Flavonoid Mucilage and Volatile oils.

Results:

Table 1: Table showing the phytochemical components screened in the plant specimens.
[+++ High color intensity; ++ Medium color intensity; + Low color intensity; - Negative color intensity].

TEST	*Azadirachta indica* (Neem)	*Ocimum sanctum* (Tulsi)	*Phyllanthus emblica* (Gooseberry)	*Citrus limon (Lemon)*	*Asparagus racemosus* (Shatavari)
Alkaloid	+	+++	++	+	+
Carbohydrate	-	+++	-	++	+
Phenolic	+++	++	-	+	-
Terpenoid	+	+	-	++	+++
Glycoside	+	++	-	+++	-
Steroid	++	+	+	-	+++
Saponin	-	-	-	-	-
Flavonoid	++	+	+++	+++	+
Mucilage	-	-	-	+	-
Volatile oil	-	-	-	+	-

Quantitative Analysis of Phytochemicals:

The total alkaloid content was determined using capsaicin as the standard (Y=0.3493x + 0.2814; R^2 =0.9889). The total amount of alkaloids were found to be 8.428, 3.882, 2.352,

3.149 and 8.694 µg/mg of sample in *Ocimum sanctum, Asparagus racemosus, Azardirachta indica, Citrus lemon and Phyllanthus emblica* respectively.

The total flavonoid content was determined using quercetin as the standard (Y=0.0063x – 0.0549; R^2 = 0.9735). The total amount of alkaloids were found to be 31.53, 32.49, 44.68, 57.56 and 61.12µg/mg of sample in *Ocimum sanctum, Asparagus racemosus, Azardirachta indica, Citrus lemon and Phyllanthus emblica* respectively.

The total phenolics content was determined using gallic acid as the standard (Y=0.0022x – 0.0664; R^2 = 0.9904). The total amount of alkaloids were found to be 22.37, 7, 74.95, 0.7 and 146.65µg/mg of sample in *Ocimum sanctum, Asparagus racemosus, Azardirachta indica, Citrus lemon and Phyllanthus emblica* respectively.

The total tannins content was determined using tannic acid as the standard (Y=0.0033x – 0.0481; R^2 = 0.9905). The total amount of alkaloids were found to be 73, 83, 3.6, 34.5 and 1.2µg/mg of sample in *Ocimum sanctum, Asparagus racemosus, Azardirachta indica, Citrus lemon and Phyllanthus emblica* respectively.

Phytochemical analysis on the leaf extracts of plants revealed that *Azadirachta indica, Ocimum sanctum* and *Citrus limon* have shown the presence of most of the tested phytochemicals. Hence, we can conclude that these plants have the better potential in the synthesis of nanoparticles.

Green synthesis of nanoparticles:

Preparation of extracts: Study specimens were washed thoroughly, peeled and cut into fine small pieces. The samples were air dried at room temperature and pulverized into fine powder using blender. The Powder suspension (1:10) was made with distilled water and

agitated at 37°C for one hour in a shaker incubator. Following filtration, the filtrate was stored and used for green synthesis with various metallic nanoparticles.

Green Synthesis of Nanoparticles: By adding 6.0 ml of either Silver Nitrate solution or CuO or ZNO (20mm) per each study with 40 ml of extract and 154 ml of deionized water was mixed in a conical flask and agitated on a magnetic stirrer depending on parameter studied such as time, Temperature and Ph the suspension was checked for the colour change. Following colour change, the contents were centrifuged at maximum speed for 15min at room temperature. The pellet obtained was washed twice with deionized water and then lyophilized to fine powder and used for further characterization.

Characterization green synthesized nanoparticles: The green synthesized metallic nanoparticles were characterized with Fourier Transform Infra-Red (FTIR), Scanning Electron Microscopy (SEM), Dynamic light scattering (DLS), UV–Vis spectrophotometry and X-ray diffraction (XRD) to study the structure, composition and morphology of the produced nanoparticles.

UV Spectroscopic analysis: Green synthesized NPs were observed for the colour change. The particles were then screened for the absorbance peak using ultraviolet-visible (UV) spectroscopy (NanoDrop ND2000, Thermo Scientific, Waltham, MA, United States; 200 to 800nm, resolution of 1nm).

From the UV spectra, all the nanoparticles synthesized from *Citrus limon* was shown to have higher absorbance, while *Phyllanthus emblica* was shown to have the least absorbance in comparison to other plant leaf extracts.

Dynamic light scattering (DLS): DLS method was used to screen for the hydrodynamic size (Z average), polydispersity index (PDI) and surface charge (zeta potential) of the green synthesized nanoparticles (Horiba SZ-100 analyzer (Kyoto, Japan). Particle size analysis was done at a scattering angle of 90° with medium count rate of 210 kCPS, at about 25°C. From the UV spectral analysis, we found significant spectral peaks for Citrus extracts.

From the DLS histogram the average particle size was found to in the range of 35-80nm with

a diffusion coefficient 6.438 x$10^{8}$$cm^{2}$/s. Silver nanoparticles peak area ranged from 35-60nm. Further they are subjected to SEM for finding the particle shape. Copper nanoparticles peak area ranged from 40-70nm. Further they are subjected to SEM for finding the particle shape. Zinc nanoparticles didn't show significant peaks within 100nm.

Figure 1: NTA analysis showing the size of (a)AgO-NPs, (b) CuO-NPs and (c) ZnO-NPs synthesized from Citrus extracts (P<0.05).

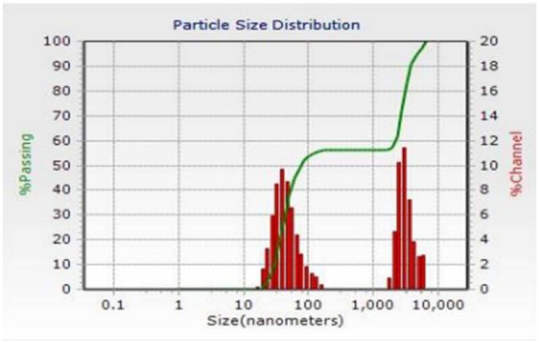

(a)

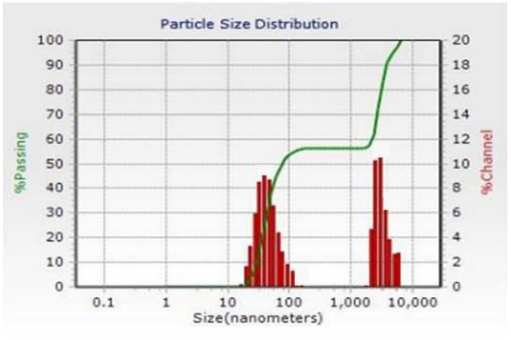

(b)

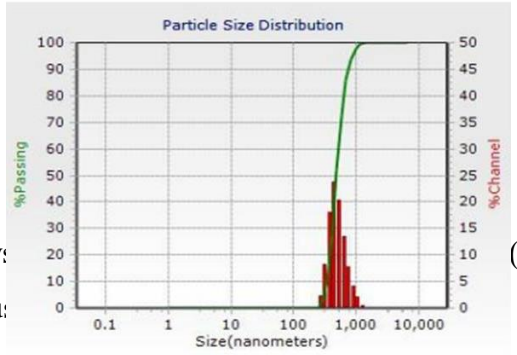

(c)

Figure 1: NTA analys (b) CuONPs and (c) ZnONPs synthesized from Citru

XRD analysis: All the three green synthesized metallic nanoparticles with Citrus extracts were used for the XRD study. From the UV spectral analysis, we found significant spectral peaks for Citrus extracts.

The XRD pattern of green synthesized AgNPs: The pattern clearly shows the main peaks at (2θ) = 27.8768 (123.19), 29.0382 (32.82), 31.5784 (44.97), 32.2985 (265.04), 33.7186 (24.69), 34.6208 (63.35), 37.0273 (49.89), 38.1909 (1135.40), 44.3518 (356.66), 46.2558 (149.77), 54.8429 (35.98), 57.5244 (42.24), 64.4805 (291.60), 67.5168 (13.81), 77.3851 (285.94). The planes of the respective peaks were shown in the brackets. Based on the XRD

spectra shown in Figure, the AgNP is likely composed of crystalline materials with a face-centered cubic (FCC) crystal structure.

The XRD pattern of green synthesized CuNPs: The pattern clearly shows the main peaks at (2θ) = 32.4039 (342.83), 35.4024 (4487.21), 38.6348 (3826.77), 44.5811 (99.71), 46.1724 (79.23), 48.6342 (1055.76), 53.3641(214.6), 58.0957 (441.58), 61.4685 (606.31), 65.9057 (649.75), 67.8711 (640.27), 72.2614 (212.09) and 75.017 (286.28). The planes of the respective peaks were shown in the brackets. Based on the XRD spectra shown in Figure 3, it appears that the CuO-NP have a face-centered cubic (FCC) crystal structure. The peak positions and intensities suggest that the particle size is relatively small.Also, it have a crystalline structure. The peaks in the spectra correspond to the diffraction of X-rays by the atoms in the crystal structure of the nanoparticles.

X-ray diffraction (XRD) of Zinc nanoparticles: The pattern clearly shows the main peaks at (2θ) = 29.3952 (135.66), 31.7617 (7443.56), 34.4218 (5069.62), 36.2460 (11935.28), 44.6126 (105.63), 47.5279 (2527.97), 56.5709 (3624.67), 62.8397 (3206.64), 66.3416 (497.54), 67.9177 (2431.46), 69.0501 (1223.00), 72.5368 (223.43), 76.9195 (420.65). The planes of the respective peaks were shown in the brackets. Based on the XRD spectra shown in Figure, Based on the XRD spectra, the main peaks observed at (2θ) the sample was crystal planes of hexagonal wurtzite ZnO, respectively. The other shape and well-defined observed indicate that the ZnONP is crystalline.

SEM: SEM was used to further determine the shape and size of the produced nanoparticles. To examine the morphological characteristics of silver, copper and Zinc nanoparticles a lyophilized sample was put under the 20kV Zeiss EVO-18 scanning electron microscope.

Scanning electron microscopy was used for the study of surface morphology of synthesized *Citrus limonum* nanoparticles. From SEM analysis, it confirmed that the green synthesized AgNPs were stabilized spherical and polydispersed with a size range of 30-70nm (mean size = 42.6nm). From SEM analysis, it was confirmed that synthesized *Citrus limonum* Copper nanoparticles showed stabilized nanocube like structure. SEM analysis confirmed that the green synthesized CuNPs were cubical and monodispersed with a size range of 40-80nm (mean size = 55.4nm).

SEM analysis confirmed that the green synthesized ZnNPs were spherical and polydispersed with a size range of more than 100nm 170-310nm (mean size = 210.8nm).

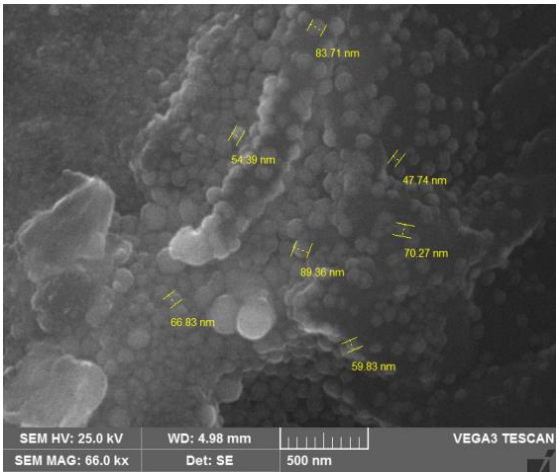

(a)

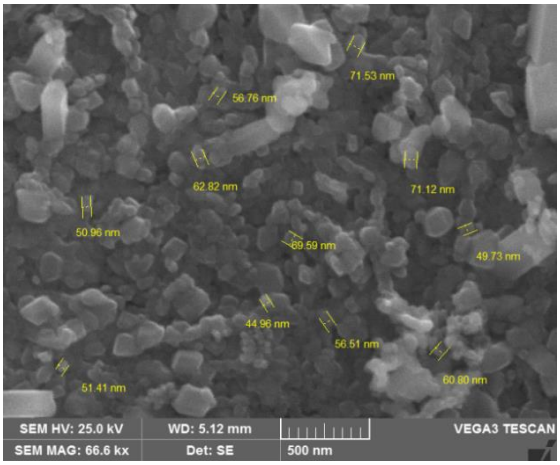

(b)

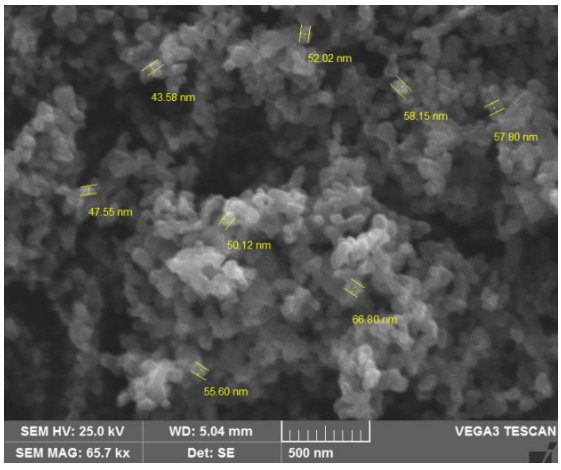

(c)

Figure 2: Images showing the SEM of the green synthesized *Citrus limonum*-nanoparticles (a) AgO-NP (a) CuO-NP (C) ZnO-NP

FTIR: To validate any effects of various phytochemicals present in the citrus fruit extract on the surface modification of the green synthesized copper nanoparticles, FTIR (JASCO Ltd., Tokyo, Japan) was done in the wavelength range of 4000-400cm^{-1}. Powdered sample was added to potassium bromide prior to evaluation.

FTIR spectra of Silver nanoparticles:

FTIR of the green synthesized AgO-NPs revealed the presence of nine bands at 492, 486, 474, 462, 455, 446, 438, 418 and 411cm^{-1}. The FTIR spectra of synthesized *Citrus limonum* nanoparticles were recorded between 500 and 400cm^{-1}. The different functional groups attached to nanoparticles were analysed by this spectroscopy. The peaks at 455.81cm^{-1} and 438.31cm^{-1} correspond to O–H bond.

FTIR spectra of Copper nanoparticles:

FTIR of the green synthesized CuO-NPs revealed the presence of nine bands at 492, 486, 467, 452, 445, 437, 428, 418 and 408cm^{-1}. The FTIR spectra of synthesized *Citrus limonum* nanoparticles were recorded between 500 and 400cm^{-1}. The different functional groups attached to nanoparticles were analyzed by this spectroscopy. The peaks at 445.23cm^{-1} and 428.81cm^{-1} correspond to O–H bond.

FTIR spectra of Zinc nanoparticles:

FTIR of the green synthesized ZnO-NPs revealed the presence of eleven bands at 500, 486, 475, 465, 455, 450, 442, 437, 419, 412 and 405cm^{-1}. The FTIR spectra of synthesized *Citrus limonum* nanoparticles were recorded between 500 and 400cm^{-1}. The different functional groups attached to nanoparticles were analyzed by this spectroscopy. The peaks at 455.11cm^{-1}

and 437.23cm^{-1} correspond to O–H bond.

Chapter 4: Method, materials and results of Screening of metal nanoparticles for anticancer activity against Leukemia.

Cell lines and culture medium:

JURKAT cell lines was procured from SKANDA life sciences cell repository stock cells were cultured in respective media supplemented with 10% inactivated Fetal Bovine Serum (FBS), penicillin (100 IU/ml), streptomycin (100 µg/ml) in a humidified atmosphere of 5% CO_2 at 37^oC until confluent.

MTT Assay: MTT assay was employed to assess the impact of green-synthesized metallic nanoparticles on cancer cell proliferation. This test utilizes MTT (3-(4,5-dimethylthazolk-2-yl)-2,5-diphenyl tetrazolium bromide), which is a quick colorimetric assay that measures the number of viable cells by cleaving its tetrazolium ring in active mitochondria of living cells.(Werner, *et al*., 2013).

IC50 Value: The half maximal inhibitory concentration (IC50) is a commonly used measure of the effectiveness of a compound in inhibiting biological or biochemical function. This quantitative measure indicates how much of a particular drug or other substance (inhibitor) is needed to inhibit a given biological process (or component of a process, i.e. an enzyme, cell, cell receptor or microorganism) by half. The lower the IC50 value, the more potent the compound is at inhibiting the target.

% Inhibition = ((OD of Control – OD of sample)/OD of Control) x 100.

Results:

The antiproliferative potential of Silver, Copper and Zinc NPs was determined by MTT assay on JURKAT cell lines. All the NPs synthesized from various plant specimens exhibited cytotoxicity to cell lines ($p<0.05$).

The NPs showed dose-dependent inhibition of cell proliferation. Interestingly, the highest toxicity was shown by *Citrus limon* samples with both Copper and Silver NPs. Among them silver showed less IC50 value which was significant when compared to positive control ($p<0.05$). IC50 of the tested silver and copper nanopartciles were found to be 43.56 µg/ml and 80.78µg/ml respectively ($p<0.05$) when compared to positive control (vincristine) (16.26µg/ml).Our results suggest that the toxicity of the AgO-NPs synthesized from *Citrus limon* to be highly specific to JURKAT cells, while the ZnO-NPs show a very less specificity.

Sl. No.	Description	IC50 values			Cell line	Method
		Ag	CuO	ZnO		
1	*Ocimum sanctum*	141.7µg/ml	>250	112.5µg/ml	JURKAT	Colorimetric Assay
2	*Asparagus racemosus*	227.4µg/ml	>250	>250		
3	*Azadirachta indica*	93.9µg/ml	105.6µg/ml	107.8µg/ml		
4	*Citrus limonum*	43.56µg/ml	80.78µg/ml	242.4µg/ml		
5	*Phyllanthus emblica*	187.1µg/ml	111.5µg/ml	>250		
6	Vincristine	16.26µM				

Table 2: Shown IC50 resultes for green synthesis nano particles

Chapter 5: Method, materials and results of Evaluation of nano-particles for

anticancer activity against Leukemia cell lines:

In this study, we characterized the synthesized nanoparticles for anticancer activity against leukaemia cell lines (Jurkat). Flow cytometric analysis was conducted to investigate cell cycle and apoptosis in Jurkat cells. Further, dual staining procedures were conducted to detect tumor cell apoptosis and to differentiate between the stages of apoptosis in Jurkat cells. Gene regulation of caspase-3, caspase-8 and p53 genes were conducted in Jurkat cells using RT-PCR, followed by western blotting technique to study the expression of proteins in Jurkat cells.

Cell Cycle studies on Jurkat cells (Jackman & O'Connor, 1998).

Results: The percentage of cells arrested in the G2/M phase of the cell cycle significantly increased from 8.48% (control) and 11.94% (40µg/ml) to 21.11% (80µg/ml) as the concentration of AgNPs increased. This difference is highly significant compared to the positive control (25.14%).

When compared to the positive control (15.58), the drug at a concentration of 80µg/ml arrested about 10.34% of cells in the S phase, while at a concentration of 40µg/ml, it arrested 5.48% of cells, and at the control concentration, it arrested 2.18% of cells.

G0/G1 was found to be 89.05 in (control) , 81.74 (40µg/ml), 68.85(80µg/ml) and 59.48 the positive control.

Sub-G0 was found to be 1.24 for the 40µg/ml stating that 1.24% of the cell population were found to be inducing apoptosis which is highly significant ($p<0.05$). while positive control Colchicine 0.26%, 80µg/ml 0.18% and the control 0.37%.

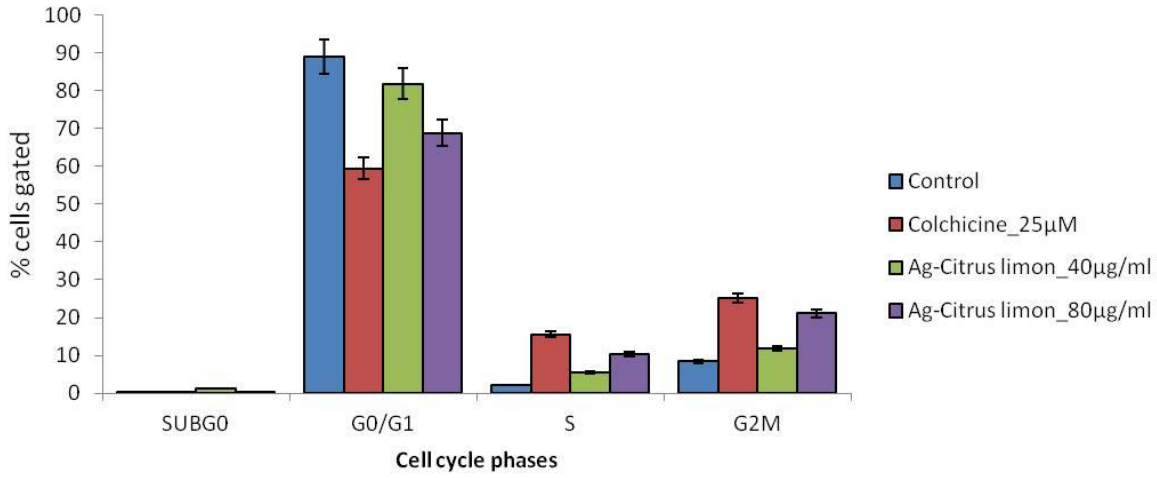

Fig 3: Flow cytometry analysis of cell cycle arrest in JURKAT cells

Apoptosis detection using PI Annexin V-FITC staining of Jurkat cells by flow cytometry (Vermes, *et al*., 1995; Koopman, *et al*., 1994).

From our results we found the percent of viability reduced from 92.13 to 63.64 at 80µg/ml which is highly significant when compared to positive control (54.12%) $P<0.05$. We also found early apoptotic cells to be increased to 12.81% from 1.35% (control). A good proportion of cells (20.91%) were pushed into late apoptosis at 80µg/ml from 2.82% (control).

FACS analysis of Apoptosis detection in JURKAT cells				
Samples	**Viable cells**	**Early Apoptotic**	**Late Apoptotic**	**Necrotic cells**
Control	92.13	1.35	2.82	3.7
Vinblastine (25µM)	54.12	18.85	25.43	1.6
Ag-*Citrus limon*_40µg/ml	73.98	11.67	12.06	2.29
Ag-*Citrus limon*_80µg/ml	63.64	12.81	20.91	2.64

Acridine Orange and Ethidium Bromide dual staining studies using Jurkat cell line (Kasibhatla, *et al*., 2006; Liu, *et al*., 2015).

Results: JURKAT cells when treated with Sample AgNPs-*Citrus limonum* at 40µg/ml showed early apoptosis and slight induction of late apoptosis. At 80µg/ml, showed higher late apoptosis and few necrotic cells also. Whereas Standard Vincristine at 25µM showed higher induction in both early and late apoptosis of JURKAT cells. ($p<0.05$).

From our results, we found a significant number of cells are stained with EtBr indicating the

necrotic stage at 80µg/ml of AgNPs treatment. Similar results are seen with Positive control but at 25µM ($p<0.05$). At 40µg/ml of treatment, more of yellow orange cells depicting the late apoptotic stages.

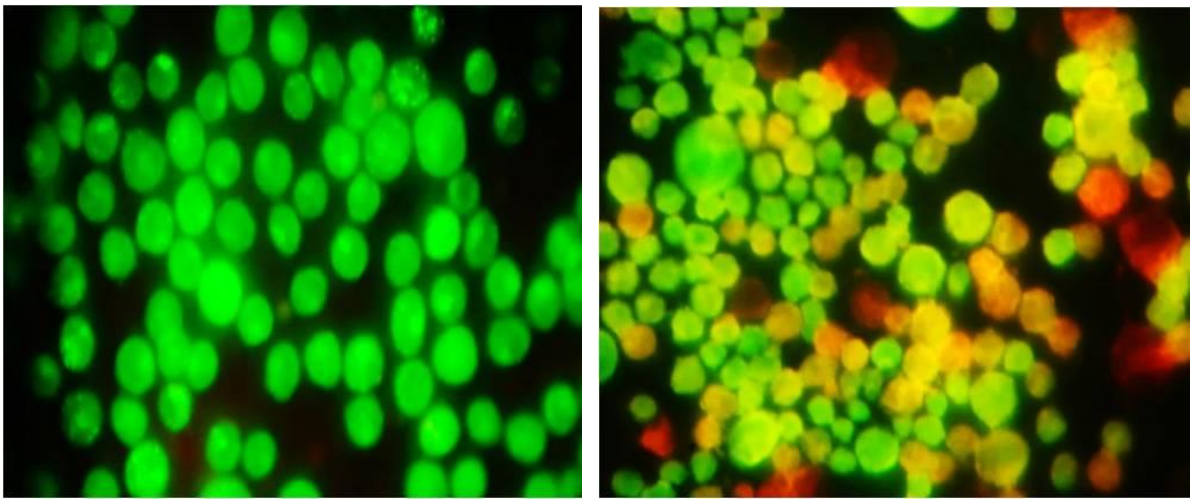

Figure 3: Acridine Orange and Ethidium Bromide dual staining studies for control Jurkat cell line. Representative images showing quantification of cell viability of control (untreated) and positive control 25µM (right). Round green cells with circular nucleus distributed in the center of the cell can be seen.

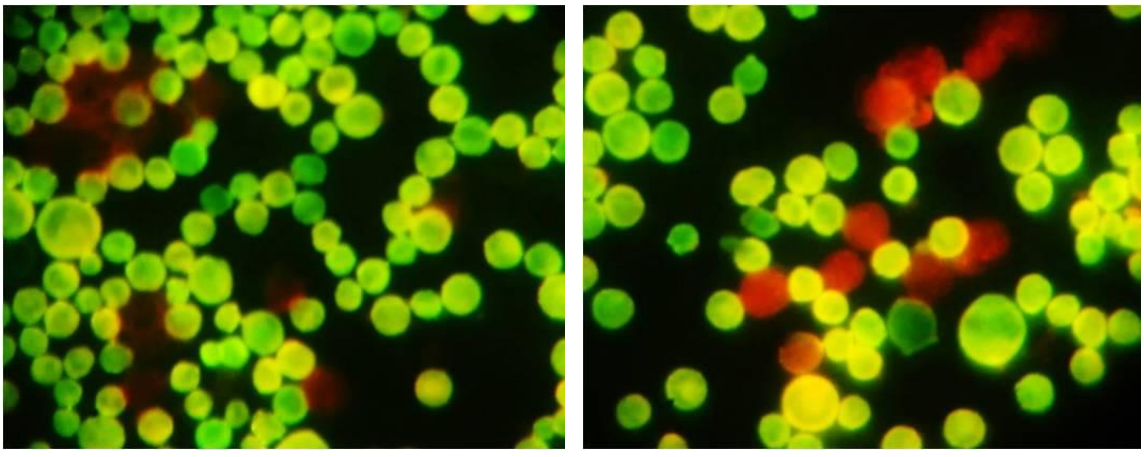

Figure 4: Acridine Orange and Ethidium Bromide dual staining studies for control Jurkat cell line. Representative images showing quantification of cell viability after 48hr of treatment with 40µg/ml and 80µg/ml (right) of AgNPs. Red cells: Cells that have taken up complete

EtBr are the necrotic cells. Green Yellow cells depict Early stage apoptotic cells.

Gene regulation of Caspase-3, Caspase-8 and P53 gene in Jurkat cells treated with sample (Schmittgen & Livak, 2008).

Calculations: Determination of relative fold expression of target gene by the Comparative CT Method ($\Delta\Delta^{Ct}$ Method) (Malla, *et al,* 2020).

Caspase 3, caspase 8 and p53 mRNA expression levels were assayed in JURKAT cells incubated with or without treatment at concentration of 40 and 80µg/ml using real time PCR method. Expression of each gene member was indicated as ratio of relative expression to that of non treated cells. Beta actin was used as house keeping gene.

The relative expression of p53 was found to be elevated to 15.51 times at 80µg/ml when compared to control (1 or 100%). On the other hand, positive control showed an elevation to 30.38 ($p<0.05$). The relative expression of Caspase -3 was found to be elevated to 3.64 times at 80µg/ml when compared to control (1 or 100%). On the other hand, positive control showed an elevation to 4.53 ($p<0.05$).

The relative expression of Caspase -3 was found to be reduced 0.22 times at 80µg/ml when compared to control (1 or 100%). On the other hand, positive control showed a reduction to 0.07 ($p<0.05$). Under expression was recorded with caspase 8 and upregulation was seen with caspase 3 and p53. The data showed that AgNPs change the regulation of apoptotic genes in JURKAT cells. We have observed more expression of caspase-3 and p53 genes and downregulation of caspase 8.

Western Blot Studies on Jurkat cells (Yang, et al.,2019). Basing on the band intensity, the relative protein expression of p53 was found to be 1.3 and 2.11 times when compared to positive control (3.74). Control expression was considered as 1 or 100%. Basing on the band

intensity, the relative protein expression of p53 was found to be 1.09 and 1.9 times when compared to positive control (3.62). Control expression was considered as 1 or 100%. Our results are in accordance to the qPCR assay.

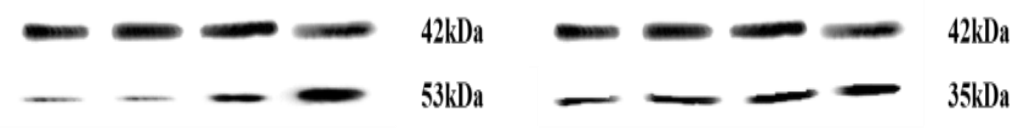

Figure 5: Western blot results showing the house keeping member and gene member. Left: p53 expression at approximately 53KDa. Right: Caspase 3 expression at approximately 35KDa.

Chapter 6: Method, materials and results of In vivo efficacy study of selected Nano-particles in Leukemia xenograft rat model.

In our study, we evaluated the possible anti-tumor efficacy of the green synthesized Silver NPs in both *in vitro* and *in vivo* models.

In vivo evaluation was studied using a xenograft model.

Treatment Groups and conditions

Once the tumour size reached the desired volume, 150mm3, tumor volumes were noted and randomly sorted into 4 groups each consisting 3 animals. Treatment groups contained, tumor control group to which normal saline was given intraperitoneally, positive control

Cyclophosphamide (CP) group received intravenously 10mg/kg and test sample treatment group III and IV received different concentration of lemon nanoparticle 40 µg/mice and 80 µg/mice i.v. respectively. The treatments schedule followed every two days once for 21 days.

Hematology study:

The blood samples were collected for a complete blood count, including erythrocytes, total leukocytes, hemoglobin, and hematocrit.

Organs evaluation parameters.

Microphotographs of Liver, Kidney, Heart ,Spleen and Lungs- shown No pathological abnormality was observed in Tumor control and Treatment groups.

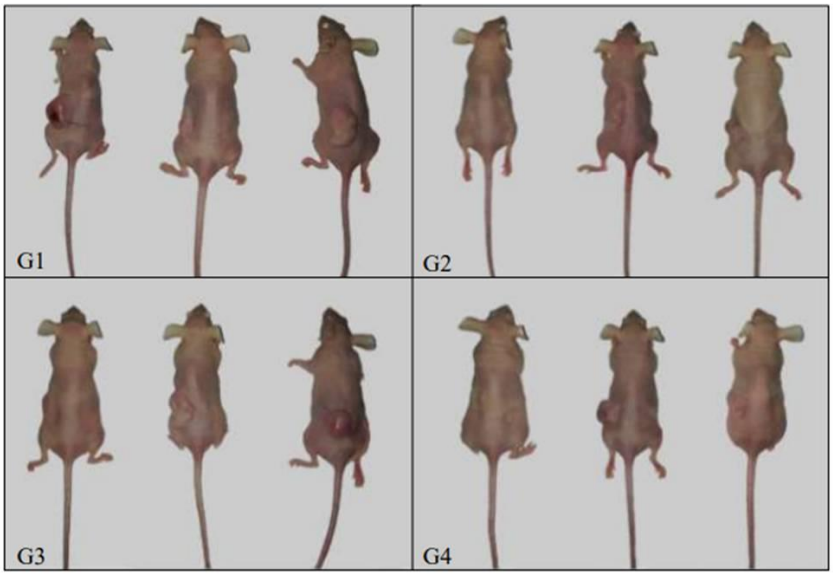

Figure 6: Photographs of the Mice bearing the tumors at the end of the treatment. Group 1, II, III, IV treated mice can be seen in the image.

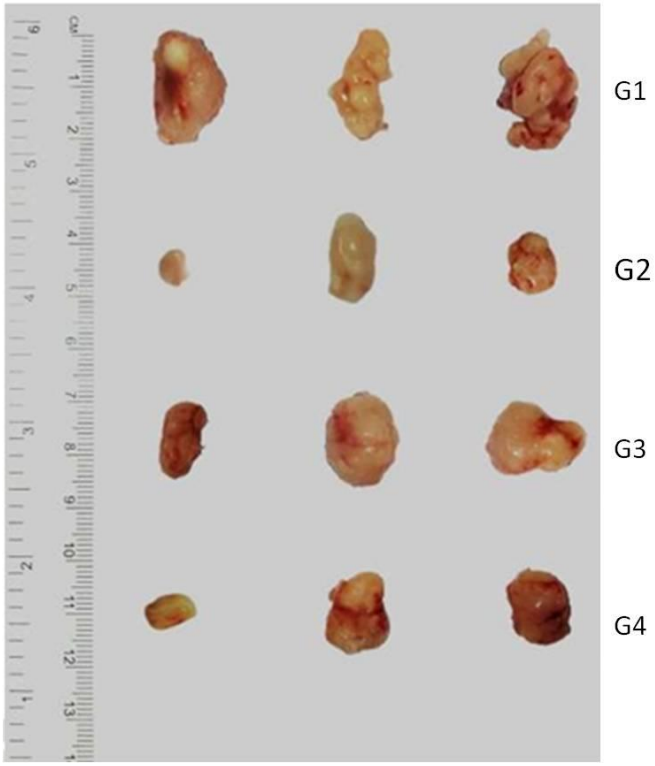

Figure 7: Photographs of the tumor resected post necroscopy. Group 1, II, III, IV treated mice can be seen in the image.

Apoptosis detection using PI and Annexin V-FITC staining of tumor cells by Flow Cytometry

From our results we found the percent of viability reduced from 82.6 to 46.09 at 80µg/ml which is highly significant when compared to positive control (34.53%) $P<0.05$. We also found early apoptotic cells to be increased to 15.38% from 6.37% (control). A good proportion of cells (27.72%) were pushed into late apoptosis at 80µg/ml from 3.18% (control). On the other hand, necrosis cells were found to be at at 80µg/ml 10.81% to 7.85% (control) ($p<0.05$).

FACS analysis of Apoptosis detection in Tumor cells				
Groups	**Viable cells**	**Early Apoptotic**	**Late Apoptoti**	**Necrotic cells**
Group 1 – Tumor control cells – Normal Saline	82.6	6.37	3.18	7.85
Group 2 – Positive Control - Cyclophosphamide (10mg/kg)	34.53	15.41	31.14	18.92
Group 3 – Lemon Nanoparticles (40µg/mice)	56.48	20.16	10.18	13.18
Group 4 – Lemon Nanoparticles (80µg/mice)	46.09	15.38	27.72	10.81

Table 4: Flow cytometry analysis of Apoptosis detection of Tumor cells

Gene regulation of Caspase-3, Caspase-8 and P53 gene in tumor tissue treated with sample

Tumor tissues Ref. Standard, NP_40µg/animal and NP_80µg/animal has showed upregulated P53 and Caspase-3 gene expression up to 6.01, 2.40, 3.68 and 5.88, 1.16, 3.41 folds when compared to Disease Control respectively. NP_40µg/animal, NP_80µg/animal and Ref. Standard tissues show downregulation of Caspase 8 expression from 0.41, 0.32 to 0.23 folds respectively.

Protein expression using western blotting.

Expression of p53, Caspase 3 and Caspase 8 in Tumor tissue:

Western blot studies on p53 and caspase-3 relative gene expression revealed higher band intensity in NP_80µg/animal as opposed to NP_40µg/animal. However, caspase-8 revealed a slightly lower band intensity in NP_80µg/animal as opposed to NP_40µg/animal.

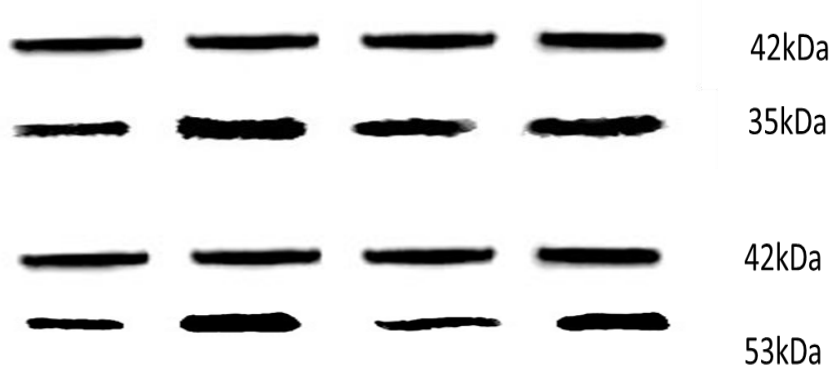

(P53)

(Casp3)

(Casp8)

Discussion:

Citrus limon, in particular its flavonoid components, have been recognised as agents with potential for use in the treatment of cancer. The anticancer potential of citrus limon syntehsized nanopartciles were presented in this study.

Citrus fruit flavonoids have been shown to influence a variety of biological processes, including cell proliferation, cell cycle regulation, apoptosis, metastasis, and angiogenesis. In recent years, molecular research has begun to clarify the fundamental cell signalling pathways that underlie the action of flavonoids. These expanding observations encourage more study of the chemopreventive potential of citrus peel extracts, and specifically isolated flavonoids (Koolaji, *et al*., 2020). In this study, we looked at the environmentally friendly manufacturing of silver and copper nanoparticles utilising natural sources, including citrus limon peel extract, and evaluated their cytotoxic and antibacterial characteristics.

From the UV spectroscopy, we found AgNPs were determined at a peak range of 420-460nm. (Kaur, et al., 2013) reported similar absorbance peaks with silver nanopartciles from Citrus. Our FTIR results predicted absorption bands in the regions of 500-400cm^{-1}. Similar bands were seen with silver nanoparticles as reported by (Alkhulaifi, *et al*., 2020). From the characterization study, we found both silver and copper nanopartciles were of nanoscale range (<100nm). Zinc NPs were exlcuded as the size was found to be more than 100nm ($p<0.05$). Silver NPs were found to spherical, and copper NPs were found to be cubical from SEM studies.

From our MTT assay on JURKAT cell lines, we found silver NPs to be highly effective in inhibiting the cell growth with a signifcant IC50 value (45.86 µg/ml). on the othe hand, IC50 of copper NPs was found to be 80.76µg/ml. Similar signficant results were reported from MTT assay. IC50 values were found to be 16.3 and 12.0µg/ml but against RAW 264.7 macrophages and MCF-7 breast cancer cells (Wypij, *et al*., 2021).

Further we planed to study only silver nanopartciles synthesized from *Citrus limon.* Basing on the MTT assay and IC50 values we further evaluated the AgNPs at 40 and 80µg/ml. Cell cycle arrest was found to be dose dependant and arrested in the G_2/M phase of the cell cycle. At this drug (80µg/ml) concentration about 10.34% of them are now arrested in the S phase when compared to positive control (15.58). Sub-G_0 was found to be 0.26 for the positive control From our results we found the percent of viability reduced from 92.13 to 63.64 at 80µg/ml which is highly significant when compared to positive control (54.12%) $P<0.05$. We also found early apoptotic cells to be increased to 12.81% from 1.35% (control). A good proportion of cells (20.91%) were pushed into late apoptosis at 80µg/ml from 2.82% (control). Numerous reports (Khane, *et al*., 2013) were publsihed on the cell cycle analysis of citrus limon synthesized nanopartciles but to our knowledge we report for the first time on JURKAT cell lines.

JURKAT cells when treated with Sample AgNPs-*Citrus limonum* at 40µg/ml showed early apoptosis and slight induction of late apoptosis. At 80µg/ml, showed higher late apoptosis and few necrotic cells also. Whereas Standard Vincristine at 25µM showed higher induction in both early and late apoptosis of JURKAT cells.

Caspase 3, caspase 8 and p53 mRNA expression levels were assayed in JURKAT cells incubated with or without treatment at concentration of 40 and 80µg/ml using real time PCR method. Expression of each gene member was indicated as ratio of relative expression to that of non treated cells. Beta actin was used as house keeping gene.

Caspase 3 was found to be upregulated on treatment with AgNPs synthesized from *Rubus fairholmianus (*Plackal, *et al*., 2018). At the same time, we also show an upregulation of p53 on treatment with AgNPs. P53 can translocate to mitochondria, interact with the antiapoptotic Bcl-2 proteins, neutralise them and cause apoptosis (Li B, *et al*., 2015).

From our results we found the percent of viability reduced from 82.6 to 46.09 at 80µg/ml which is highly significant when compared to positive control (34.53%) $P<0.05$.

We also found early apoptotic cells to be increased to 15.38% from 6.37% (control). A good proportion of cells (27.72%) were pushed into late apoptosis at 80µg/ml from 3.18% (control). On the other hand, necrosis cells were found to be at 10.81% from 7.85% ($p<0.05$).

The AO/EB fluorescence microscopic staining assay was used to observe the morphological changes in JURKAT cells. We found that the control cells did not change and the cell remains green after staining, whereas the color of the treated cells changed (orange), indicating the apoptotic cells. Similar results were seen in case of MCF-7 cell lines when treated with *Fagonia indica* (Ullah, *et al*., 2020).

Tumor tissues Ref. Standard, NP_40µg/animal and NP_80µg/animal has showed upregulated P53 and Caspase-3 gene expression up to 6.01, 2.40, 3.68 and 5.88, 1.16, 3.41 folds when compared to Disease Control respectively. NP_40µg/animal, NP_80µg/animal and Ref. Standard tissues show downregulation of Caspase 8 expression from 0.41, 0.32 to 0.23 folds respectively. Western blot studies on p53 and caspase-3 relative gene expression revealed higher band intensity in NP_80µg/animal as opposed to NP_40µg/animal. However, caspase-8 revealed a slightly lower band intensity in NP_80µg/animal as opposed to NP_40µg/animal.

The same type of membrane changes was observed in MCF-7-treated cells of *Morinda pubescens*-synthesized Silver nanoparticles (Inbathamizh,*etal*.,2013), *Teucrium stocksianum* extract-mediated AgNPs, *Syzygium aromaticum* extract-mediated AgNPs, and *Solanum trilobatum* fruit extract silver nanoparticles (Ramar, *et al*., 2015).

Key findings:

Objective 1:

- We found *Citrus lemon* to be highly loaded with phytochemcials and showed maximum absorption with all three metallic nanopartciles.
- From the characterization study, we found both silver and copper nanopartciles were of nanoscale range (<100nm).
- Silver NPs were found to spherical, and copper NPs were found to be cubical from SEM studies.

Objective 2:

- From the MTT assay studied using JURKAT cell lines, we found silver NPs were found to have lower IC50 value (45.86) than copper NPs (80.76).

Objective 3:

- Cell cycle arrest was found to be dose dependant and arrested in the G_2/M phase of the cell cycle.
- From our results we found the percent of viability reduced from 92.13 to 63.64 at 80µg/ml which is highly significant when compared to positive control (54.12%) $P<0.05$.
- We also found early apoptotic cells to be increased to 12.81% from 1.35% (control).
- A good proportion of cells (20.91%) were pushed into late apoptosis at 80µg/ml from 2.82% (control).
- JURKAT cells when treated with Sample AgNPs-*Citrus limonum* at 40µg/ml showed early apoptosis and slight induction of late apoptosis.
- We found upregulation of both p53 and Caspase 3 gene members when compared to their controls.
- Protein expression as seen on western blot confirmed the upregulation of the gene members.

Objective 4:

- From our results we found the percent of viability reduced from 82.6 to 46.09 at 80µg/ml which is highly significant when compared to positive control (34.53%) $P<0.05$.
- Standard tissues showed downregulation of Caspase 8 expression from 0.41, 0.32 to 0.23 folds respectively.
- Western blot studies on p53 and caspase-3 relative gene expression revealed higher band intensity in NP_80µg/animal as opposed to NP_40µg/animal.

Conclusion:

In this study, we report a one-step biosynthesis of ecofriendly and stable metallic NPs from various plant samples. Furthermore, controlled size nanoparticles (40-70nm) were obtained that were confirmed by XRD, DLS, and SEM analyses. The *Citrus limon* extract synthesized AgNPs induced anticancer activity in a concentration-dependent manner. The NPs induced apoptotis due to activation of caspases.

In summary, our data indicated that the biosynthesized Ag-NPs induced apoptosis on JURKAT cell line, which was confirmed using AO/Et and DAPI staining. Caspase-3, p53

and caspase 8 activities showed that the cell death involved a caspase dependant intracellular pathway. Biosynthesized Ag-NPs from *Citrus limon* could be considered a potential chemotherapeutic agent in the treatment of leukemia and other related cancers.

Future studies:

Basing on the promising results we got from our study, we further planned to purify the phytochemical compunds and investigate their role as antincaerous agents. Purification of the compounds by GCMS and HPLC would be carried out. We also would like to extend the study not to one cell line but to confirm the positive findings with 3 other cell lines.

Additionally, studies may also, focus on optimizing the biosynthesis process to improve the yield, stability, and reproducibility of the NPs.

Paper published:-

1. Huda Jameel Makki and Dr. K S Chandrashekaraiah "The impact of using Citrus limonumZinc-nano particles against leukemia cells". IJFANS INTERNATIONAL JOURNAL OF FOOD AND NUTRITIONAL SCIENCES. 2022; Volume 11 , Issue - 12 : Page: 2962-2972.
   0d92c85eedeb6dea9a963de7f70f0d05.pdf (ijfans.org)

2. Huda Jameel Makki and Dr. K S Chandrashekaraiah "Synthesis and Characterization of Citrus limonum Copper Nanoparticles and Its In Vitro Evaluation of Cytotoxicity Against JURKAT Cells". Pharmacognosy Magazine.
   https://doi.org/10.1177/0973129623117749

References:

1. Alkhulaifi, M. M., Alshehri, J. H., Alwehaibi, M. A., Awad, M. A., Al-Enazi, N. M., Aldosari, N. S., ... & Abdel-Raouf, N. (2020). Green synthesis of silver nanoparticles using Citrus limon peels and evaluation of their antibacterial and cytotoxic properties. Saudi Journal of Biological Sciences, 27(12), 3434-3441.

2. Ajanal, M., Gundkalle, M. B., & Nayak, S. U. (2012). Estimation of total alkaloid in Chitrakadivati by UV-Spectrophotometer. Ancient science of life, 31(4), 198.

3. Bhat, R. S., Almusallam, J., Al Daihan, S., & Al-Dbass, A. (2019). Biosynthesis of silver nanoparticles using Azadirachta indica leaves: characterisation and impact on Staphylococcus aureus growth and glutathione-S-transferase activity. IET Nanobiotechnology, 13(5), 498-502.

4. Bray, F., Ferlay, J., Soerjomataram, I., Siegel, R. L., Torre, L. A., & Jemal, A. (2018). Global cancer statistics 2018: GLOBOCAN estimates of incidence and mortality worldwide for 36 cancers in 185 countries. CA: a cancer journal for clinicians, 68(6), 394-424.

5. Chiang, K. W., Noureldin, A., & El-Sheimy, N. (2004). A new weight updating method for INS/GPS integration architectures based on neural networks. Measurement Science and Technology, 15(10), 2053.

6. Ghozali, S. Z., Vuanghao, L., & Ahmad, N. H. (2015). 'Biosynthesis and characterization of silver nanoparticles using Catharanthus roseus leaf extract and its proliferative effects on cancer cell lines. J Nanomed Nanotechnol 6: 305. C. roseus. S. Z., Vuanghao, L., & Ahmad, N. H. (2015). 'Biosynthesis and characterization of silver nanoparticles using Catharanthus roseus leaf extract and its proliferative effects on cancer cell lines. J Nanomed Nanotechnol 6: 305. C. roseus.

7. Gwinn, M. R., & Vallyathan, V. (2006). Nanoparticles: health effects—pros and cons. Environmental health perspectives, 114(12), 1818-1825.

8. Inbathamizh, L., Ponnu, T. M., & Mary, E. J. (2013). In vitro evaluation of antioxidant and anticancer potential of Morinda pubescens synthesized silver nanoparticles. Journal of Pharmacy Research, 6(1), 32-38.

9. Jackman, J., & O'Connor, P. M. (1998). Methods for synchronizing cells at specific stages of the cell cycle. Current protocols in cell biology, (1), 8-3.

10. Juliusson, G., Lazarevic, V., Hörstedt, A. S., Hagberg, O., & Höglund, M. (2012). Acute myeloid leukemia in the real world: why population-based registries are needed. Blood, The Journal of the American Society of Hematology, 119(17), 3890-3899.

11. Kalpana, V. N., Kataru, B. A. S., Sravani, N., Vigneshwari, T., Panneerselvam, A., & Rajeswari, V. D. (2018). Biosynthesis of zinc oxide nanoparticles using culture filtrates of Aspergillus niger: Antimicrobial textiles and dye degradation studies. OpenNano, 3, 48-55.

12. Kasibhatla, S., Amarante-Mendes, G. P., Finucane, D., Brunner, T., Bossy-Wetzel, E., & Green, D. R. (2006). Acridine orange/ethidium bromide (AO/EB) staining to detect apoptosis. Cold Spring Harbor Protocols, 2006(3), pdb-prot4493.

13. Kaur, P., Choudhary, A., & Thakur, R. (2013). Synthesis of chitosan-silver nanocomposites and their antibacterial activity. Int J Sci Eng Res, 4(4), 869.

14. Khane, Y., Benouis, K., Albukhaty, S., Sulaiman, G. M., Abomughaid, M. M., Al Ali, A., ... & Dizge, N. (2022). Green synthesis of silver nanoparticles using aqueous Citrus limon zest extract: Characterization and evaluation of their antioxidant and antimicrobial properties. Nanomaterials, 12(12), 2013.

15. Kojima, K., Konopleva, M., Samudio, I. J., Shikami, M., Cabreira-Hansen, M., McQueen, T., ... & Andreeff, M. (2005). MDM2 antagonists induce p53-dependent apoptosis in AML: implications for leukemia therapy. Blood, 106(9), 3150-3159.

16. Koolaji, N., Shammugasamy, B., Schindeler, A., Dong, Q., Dehghani, F., & Valtchev, P. (2020). Citrus peel flavonoids as potential cancer prevention agents. Current developments in nutrition, 4(5), nzaa025.

17. Koopman, G., Reutelingsperger, C. P., Kuijten, G. A., Keehnen, R. M., Pals, S. T., & Van Oers, M. H. (1994). Annexin V for flow cytometric detection of phosphatidylserine expression on B cells undergoing apoptosis.

18. Kumar, D., Jamwal, A., Madaan, R., & Kumar, S. (2014). Estimation of total phenols and flavonoids in selected Indian traditional plants. Journal of Pharmaceutical Technology, Research and Management, 2(1), 77-86.

19. Kumarasamyraja, D., & Jeganathan, N. S. (2013). Green synthesis of silver nanoparticles using aqueous extract of acalypha indica and its antimicrobial activity. Int J Pharm Bio Sci, 4(3), 469-476.

20. Li, B., Gao, Y., Rankin, G. O., Rojanasakul, Y., Cutler, S. J., Tu, Y., & Chen, Y. C. (2015). Chaetoglobosin K induces apoptosis and G2 cell cycle arrest through p53-dependent pathway in cisplatin-resistant ovarian cancer cells. Cancer letters, 356(2), 418-433.

21. Liu, K., Liu, P. C., Liu, R., & Wu, X. (2015). Dual AO/EB staining to detect apoptosis in osteosarcoma cells compared with flow cytometry. Medical science monitor basic research, 21, 15.

22. Malla Sudhakar and B. Venkata Raman, 2020. Bactericidal and Anti-biofilm Activity of Tannin Fractions Derived from Azadirachta against Streptococcus mutans. Asian Journal of Applied Sciences, 13: 132-143.DOI: 10.3923/ajaps.2020.132.143

23. Mathers, C. D., Boschi-Pinto, C., Lopez, A. D., Murray, C. J., & World Health Organization. (2001). Cancer incidence, mortality and survival by site for 14 regions of the world.

24. Madhu, M., Sailaja, V., Satyadev, T. N. V. S. S., & Satyanarayana, M. V. (2016). Quantitative phytochemical analysis of selected medicinal plant species by using various organic solvents. Journal of pharmacognosy and phytochemistry, 5(2), 25-29.

25. Muniyappan, N., Pandeeswaran, M., & Amalraj, A. (2021). Green synthesis of gold nanoparticles using Curcuma pseudomontana isolated curcumin: Its characterization, antimicrobial, antioxidant and anti-inflammatory activities. Environmental Chemistry and Ecotoxicology, 3, 117-124.

26. Najahi-Missaoui, W., Arnold, R. D., & Cummings, B. S. (2020). Safe nanoparticles: Are we there yet?. International Journal of Molecular Sciences, 22(1), 385.

27. Naumburg, E., Bellocco, R., Cnattingius, S., Jonzon, A., & Ekbom, A. (2002). Perinatal exposure to infection and risk of childhood leukemia. Medical and pediatric oncology, 38(6), 391-397.

28. Plackal Adimuriyil George, B., Kumar, N., Abrahamse, H., & Ray, S. S. (2018). Apoptotic efficacy of multifaceted biosynthesized silver nanoparticles on human adenocarcinoma cells. Scientific reports, 8(1), 14368.

29. Ramar, M., Manikandan, B., Marimuthu, P. N., Raman, T., Mahalingam, A., Subramanian, P., ... & Munusamy, A. (2015). Synthesis of silver nanoparticles using Solanum trilobatum fruits extract and its antibacterial, cytotoxic activity against human breast cancer cell line MCF 7. Spectrochimica Acta Part A: Molecular and Biomolecular Spectroscopy, 140, 223-228.

30. Siddiqi, K. S., Husen, A., & Rao, R. A. (2018). A review on biosynthesis of silver nanoparticles and their biocidal properties. Journal of nanobiotechnology, 16(1), 1-28.

31. Vermes, I., Haanen, C., Steffens-Nakken, H., & Reutellingsperger, C. (1995). A novel assay for apoptosis flow cytometric detection of phosphatidylserine expression on early apoptotic cells using fluorescein labelled annexin V. Journal of immunological methods, 184(1), 39-51.

32. Ullah, I., Khalil, A. T., Ali, M., Iqbal, J., Ali, W., Alarifi, S., & Shinwari, Z. K. (2020). Green-synthesized silver nanoparticles induced apoptotic cell death in MCF-7 breast cancer cells by generating reactive oxygen species and activating caspase 3 and 9 enzyme activities. Oxidative medicine and cellular longevity, 2020.

33. Werner, M., Biss, K., Jérôme, V., Hilbrig, F., Freitag, R., Zambrano, K., ... & Wandrey, C. (2013). Use of the mitochondria toxicity assay for quantifying the viable cell density of microencapsulated jurkat cells. Biotechnology Progress, 29(4), 986-993.

34. Wypij, M., Jędrzejewski, T., Trzcińska-Wencel, J., Ostrowski, M., Rai, M., & Golińska, P. (2021). Green synthesized silver nanoparticles: antibacterial and anticancer activities, biocompatibility, and analyses of surface-attached proteins. Frontiers in microbiology, 12, 632505.

35. Xu, Z., Wang, H., Wei, S., Wang, Z., & Ji, G. (2018). Inhibition of ER stress-related IRE1α/CREB/NLRP1 pathway promotes the apoptosis of human chronic myelogenous leukemia cell. Molecular immunology, 101, 377-385.

36. Yang, R., Jia, Q., Ma, S. F., Wang, Y., Mehmood, S., & Chen, Y. (2019). Exogenous H2S mitigates myocardial fibrosis in diabetic rats through suppression of the canonical Wnt pathway. International journal of molecular medicine, 44(2), 549-558.

Declaration:

This is to certify that the work in the report "Green synthesis of Nano-particles using medicinal plants and evaluation for anti-cancer activity against Leukemia cells" has been carried out by Huda Jameel Makki, under the supervision Prof. K S Chandrashekaraiah (Dep. of Biochemistry PG Centre, Jnana Kaveri Campus, Chikka Aluvara. Mangalore University. It is further certified that no reearch work under this heading has previously been submitted to the Mangalore University or any other institution for any degree, to the best of our belief.

Ph.D Scholar **Research Supervisor**

Chairman

DOS in Biochemistry

Date: 30/08/ 2022